

# Carbon Miscibility in the Boron Layers of the MgB<sub>2</sub> Superconductor

I. Maurin,<sup>†</sup> S. Margadonna,<sup>\*,‡</sup> K. Prassides,<sup>\*,†</sup> T. Takenobu,<sup>§,||</sup> Y. Iwasa,<sup>§,||</sup> and A. N. Fitch<sup>⊥</sup>

*School of Chemistry, Physics and Environmental Science, University of Sussex, Brighton BN1 9QJ, United Kingdom, Department of Chemistry, University of Cambridge, Cambridge CB2 1EW, United Kingdom, Institute for Materials Research, Tohoku University, 2-1-1 Katahira, Aoba-ku, Sendai 980-8577, Japan, CREST, Japan Science and Technology Corporation, Kawaguchi 332-0012, Japan, and European Synchrotron Radiation Facility, BP 220, 38042 Grenoble, France*

Received March 29, 2002. Revised Manuscript Received July 23, 2002

A detailed structural analysis of the MgB<sub>2-x</sub>C<sub>x</sub> series at low doping levels ( $0 \leq x \leq 0.1$ ) is presented. High-resolution synchrotron X-ray powder diffraction experiments show an extremely small miscibility of carbon within the boron sheets despite the structural analogy between MgB<sub>2</sub> and graphite. Multiphase behavior is detected for  $x \geq 0.04$ . The coexisting phases, isostructural with the parent MgB<sub>2</sub> compound, differ mainly in their in-plane lattice constants, as evidenced by the splitting of the (hk0) Bragg reflections. All phases contain carbon in substitution for boron but in different concentrations.

## 1. Introduction

Discovery of superconductivity at 39 K in the simple MgB<sub>2</sub> compound<sup>1</sup> has stimulated a lot of experimental and theoretical work during the past year. The unexpectedly high critical temperature reported is close to the upper limit predicted for BCS-type superconductivity. A conventional phonon-mediated pairing mechanism in this material is supported by the observation of a significant boron isotope effect,<sup>2</sup> scanning tunneling experiments,<sup>3,4</sup> and decreased  $T_c$  values under hydrostatic pressure.<sup>5–7</sup> The low mass of boron, leading to high phonon frequencies, should be responsible for such a high  $T_c$ , as supported by band structure and phonon calculations. The charge carriers are situated in two bands derived from the  $\sigma$ -bonding p<sub>x,y</sub> orbitals of boron, which are essentially two-dimensional (2D), and in one electron and one hole bands derived from the  $\pi$ -bonding p<sub>z</sub> orbitals of boron.<sup>8</sup> There is general agreement that a key point for superconductivity in MgB<sub>2</sub> is the 2D  $\sigma$  band

of p<sub>x,y</sub> orbitals within the boron layers. Consistent with these theoretical expectations, precise structural information has revealed an extremely small discontinuity in the boron interlayer spacing near  $T_c$ .<sup>9</sup>

In this context, the change in carrier concentration through chemical substitution within or in between the boron layers is of particular interest. Up until now, several ternary compositions have been prepared for electron (Mg<sub>1-x</sub>Al<sub>x</sub>B<sub>2</sub><sup>10</sup> and MgB<sub>2-x</sub>C<sub>x</sub><sup>11,12</sup>), hole (Mg<sub>1-x</sub>Li<sub>x</sub>B<sub>2</sub><sup>13</sup>), and isovalent (Mg<sub>1-x</sub>Mn<sub>x</sub>B<sub>2</sub><sup>14</sup> and Mg<sub>1-x</sub>Zn<sub>x</sub>B<sub>2</sub><sup>15</sup>) doping of MgB<sub>2</sub>, all resulting in decreased  $T_c$ 's. For most of the doped samples, a broadening of the diffraction lines with increased intra- or interlayer substitution is evident by laboratory X-ray diffraction experiments, indicating loss of crystallinity associated with structural disorder, phase separation, or more complex structural phenomena, e.g., ordering of the dopants as reported for certain Mg<sub>1-x</sub>Al<sub>x</sub>B<sub>2</sub> phases.<sup>16,17</sup> Hence, the observed decrease in  $T_c$  may not only reflect a change in the charge-carrier density but also partly arise from inho-

\* To whom correspondence should be addressed: (S.M.) sm413@cam.ac.uk; (K.P.) K.Prassides@susx.ac.uk.

<sup>†</sup> University of Sussex.

<sup>‡</sup> University of Cambridge.

<sup>§</sup> Tohoku University.

<sup>||</sup> CREST, Japan Science and Technology Corp.

<sup>⊥</sup> European Synchrotron Radiation Facility.

(1) Nagamatsu, J.; Nakagawa, N.; Muranaka, T.; Zenitani, Y.; Akimitsu, J. *Nature* **2001**, *410*, 63.

(2) Bud'ko, S. L.; Lapertot, G.; Petrovic, C.; Cunningham, C. E.; Anderson, N.; Canfield, P. C. *Phys. Rev. Lett.* **2001**, *86*, 1877.

(3) Karapetrov, G.; Iavarone, M.; Kwok, W. K.; Crabtree, G. W.; Hinks, D. G. *Phys. Rev. Lett.* **2001**, *86*, 4374.

(4) Sharoni, A.; Felner, I.; Millo, O. *Phys. Rev. B* **2001**, *63*, 22508.

(5) Monteverde, M.; Nunez-Regueiro, M.; Rogado, N.; Regan, K. A.; Hayward, M. A.; He, T.; Loureiro, S. M.; Cava, R. J. *Science* **2001**, *292*, 75.

(6) Lorenz, B.; Meng, R. L.; Chu, C. W. *Phys. Rev. B* **2001**, *64*, 12507.

(7) Saito, E.; Takenobu, T.; Ito, T.; Iwasa, Y.; Prassides, K.; Arima, T. *J. Phys.: Condens. Matter* **2001**, *13*, L267.

(8) Kortus, J.; Mazin, I. I.; Belaschenko, K. D.; Antropov, V. P.; Boyer, L. L. *Phys. Rev. Lett.* **2001**, *86*, 4656. An, J. M.; Pickett, W. E. *Phys. Rev. Lett.* **2001**, *86*, 4366.

(9) Margadonna, S.; Muranaka, T.; Prassides, K.; Maurin, I.; Brigatti, K.; Ibbsen, R. M.; Arai, M.; Takata, M.; Akimitsu, J. *J. Phys.: Condens. Matter* **2001**, *13*, L795.

(10) Slusky, J. S.; Rogado, N.; Regan, K. A.; Hayward, M. A.; Khalifa, P.; He, T.; Inumaru, K.; Loureiro, S. M.; Haas, M. K.; Zandbergen, H.; Cava, R. J. *Nature* **2001**, *410*, 343.

(11) Takenobu, T.; Ito, T.; Chi, D. H.; Prassides, K.; Iwasa, Y. *Phys. Rev. B* **2001**, *64*, 134513.

(12) Bharathi, A.; Balaselvi, S. J.; Kalavathi, S.; Reddy, G. L. N.; Sastry, V. S.; Hariharan, Y.; Radhakrishnan, T. S. *Physica C* **2002**, *370*, 211.

(13) Zao, Y. G.; Zhang, X. P.; Qiao, P. T.; Zhang, H. T.; Jia, S. L.; Cao, B. S.; Zhu, M. H.; Han, Z. H.; Wang, X. L.; Gu, B. L. *Physica C* **2001**, *361*, 91.

(14) Xu, S.; Moritomo, Y.; Kato, K.; Nakamura, A. *J. Phys. Soc. Jpn.* **2001**, *70*, 1889.

(15) Kazakov, S. M.; Angst, M.; Karpinski, J.; Fita, I. M.; Puzniak, R. *Solid State Commun.* **2001**, *119*, 1.

(16) Zandbergen, H. W.; Wu, M. Y.; Jiang, H.; Hayward, M. A.; Haas, M. K.; Cava, R. J. *Physica C* **2002**, *366*, 221.

(17) Margadonna, S.; Prassides, K.; Arvanitidis, I.; Pissas, M.; Papavassiliou, G.; Fitch, A. N. *Phys. Rev. B* **2002**, *66*, 014158.

mogeneity effects. High-resolution structural analyses are, therefore, clearly needed to draw reliable conclusions on the structural effects associated with the doping. In addition, earlier work has shown that non-stoichiometry and chemical inhomogeneities are often present even in undoped  $MgB_2$  samples,<sup>18</sup> resulting in a pressure dependence of the electrical resistivity and superconducting transition temperature, which is strongly sample-dependent.<sup>5</sup> High-resolution powder neutron diffraction data have also provided clear evidence for temperature-independent multiphase behavior, which was modeled by coexisting  $Mg_{1+\delta}B_2$  phases.<sup>9</sup>

The  $MgB_2$  crystal structure consists of alternating close-packed  $Mg^{2+}$  layers and honeycomblike boron sheets.<sup>19</sup> Because of the similarity between graphite and the boron layers in  $MgB_2$ , carbon substitution for boron might be expected to lead to extended solid solution behavior. However, single-phase samples were only encountered for a relatively small range of nominal carbon concentrations,  $x < 0.10$ .<sup>11</sup>  $T_c$  was found to gradually decrease upon substitution, consistent with a decrease in the density of states at the Fermi level induced by both electron doping and reduced lattice volume,<sup>11</sup> as predicted by the results of band structure calculations<sup>8</sup> and high-pressure experiments,<sup>5–7</sup> respectively. In the present work, we have used high-resolution synchrotron X-ray powder diffraction techniques to investigate in detail the structural changes associated with intralayer carbon doping. We find that the miscibility limit of carbon in  $MgB_2$  for the present preparative conditions is very small and that, at doping levels of  $x > 0.04$ , two or more phases with the same  $AlB_2$ -type crystal structure but differing in-plane lattice constants (and carbon contents) coexist.

## 2. Experimental Section

The  $MgB_{2-x}C_x$  ( $x = 0, 0.02, 0.04, 0.06, 0.08$ , and  $0.10$ ) sample preparation is described in ref 11. Laboratory X-ray powder diffraction measurements at room temperature showed that the intralayer lattice parameter,  $a$ , decreases linearly with carbon substitution, while the interlayer separation,  $c$ , remains nearly constant, suggesting that carbon is only introduced in the boron layers.<sup>11</sup> High-resolution synchrotron X-ray diffraction experiments on the same samples were carried out on the BM16 beamline at the European Synchrotron Radiation Facility, France. Samples were sealed in 0.5-mm-diameter glass capillaries, and diffraction profiles ( $\lambda = 0.6889$  Å) were collected at room temperature and 16 K in continuous scanning mode using nine Ge(111) analyzer crystals. The capillaries were continuously spun during data acquisition. The data were rebinned in the  $2\theta$  range of  $1$ – $88^\circ$  to a step of  $0.01^\circ$  and refined using the GSAS suite of Rietveld analysis programs.<sup>20</sup> Because of the poor contrast between boron and carbon X-ray scattering factors, we constrained the composition of all phases to be  $MgB_{2+\delta}$ . Electron doping, associated with carbon substitution, is thus expressed as an occupancy on the boron sites of slightly larger than 100%. The diffraction lines were modeled by a pseudo-Voigt function, and the Lorentzian contribution to the peak shape was empirically taken as  $(X - X_e \cos \phi)/\cos \theta + (Y - Y_e \cos \phi) \tan \theta$ .<sup>21</sup> Strain effects, induced by stacking faults and dislocations in the basal  $a$ – $b$  planes,<sup>22,23</sup> substantially broaden the  $(hk0)$  Bragg reflections. Anisotropic broadening

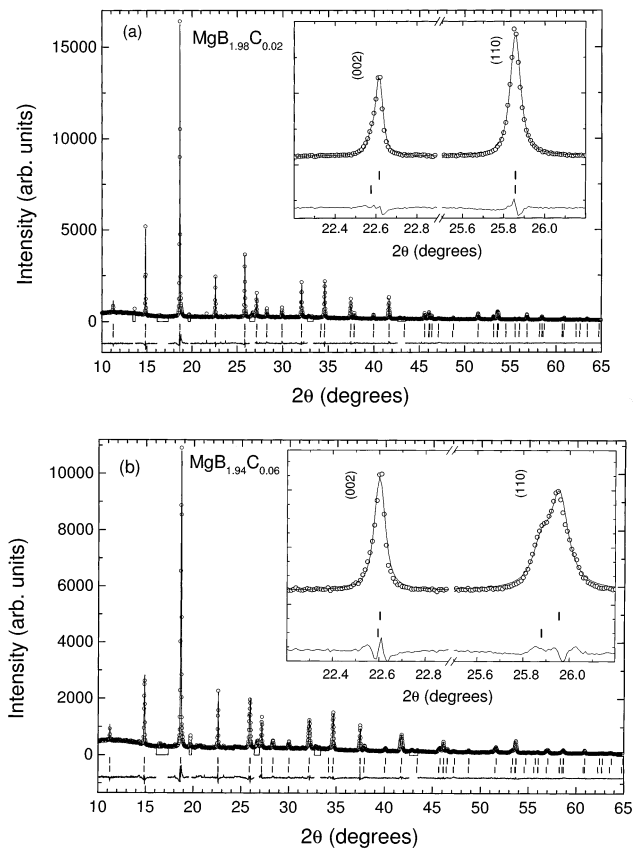


**Figure 1.** Observed (open circles) and calculated (solid line) synchrotron X-ray diffraction profiles for  $MgB_{1.98}C_{0.02}$  (a) and  $MgB_{1.94}C_{0.06}$  (b) at 16 K ( $\lambda = 0.6889$  Å). In each case, the lower solid line shows the difference profile and the tick marks show the reflection positions. Impurity peaks arising from  $MgO$  were excluded from the refinements. Insets: enlarged views of the (002) and (110) lines.

terms,  $X_e$  and  $Y_e$ , were therefore required to reproduce the relative sharpness of the  $(00l)$  lines.  $\phi$  represents the angle between the scattering vector  $[hkl]$  and the anisotropic axis,  $[001]$ .

## 3. Results and Discussion

The diffraction profiles of the  $MgB_2$  and  $MgB_{1.98}C_{0.02}$  samples were refined assuming the  $AlB_2$ -type crystal structure,  $P6/mmm$  space group, initially proposed by Jones et al.<sup>19</sup> Shoulders are apparent on the low-angle side of the  $(00l)$  Bragg reflections (inset of Figure 1a). This asymmetric line shape has been previously reported from high-resolution neutron diffraction data<sup>9</sup> and empirically modeled by the coexistence of phases (or intergrowths) showing a range of discrete (or a continuum) of interlayer separations. Such a distribution in  $c$  spacings may be accounted for by edge dislocations in the form of additional  $Mg$  or  $B$  planes, which might be present in the stacking sequences, as discussed by Zhu et al. from transmission electron microscopy experiments.<sup>22</sup> To get unbiased sets of lattice parameters, this particular peak shape was empirically

(18) Zhao, Y. G.; Zhang, X. P.; Qiao, P. T.; Zhang, H. T.; Jia, S. L.; Cao, B. S.; Zhu, M. H.; Han, Z. H.; Wang, X. L.; Gu, B. L. *Physica C* **2001**, *366*, 1.

(19) Jones, M. E.; Marsh, R. E. *J. Am. Chem. Soc.* **1954**, *76*, 1434.

(20) Larsen, A. C.; von Dreele, R. B. GSAS software, Los Alamos National Laboratory Report No. LAUR 86-748.

(21) Thompson, P. E.; Cox, D. E.; Hastings, J. B. *J. Appl. Crystallogr.* **1987**, *20*, 79. Finger, L. W.; Cox, D. E.; Jephcoat, A. P. *J. Appl. Crystallogr.* **1994**, *27*, 892.

(22) Zhu, Y.; Wu, L.; Volkov, V.; Li, Q.; Gu, G.; Moomenbaugh, A. R.; Malac, M.; Suenaga, M.; Tranquada, J. *Physica C* **2001**, *356*, 239.

(23) Li, J. Q.; Li, L.; Zhou, Y. Q.; Ren, Z. A.; Che, G. C.; Zhao, Z. X. *Chin. Phys. Lett.* **2001**, *18*, 380.

**Table 1. Refined Parameters for  $MgB_{2-x}C_x$  at 16 K in the Space Group  $P6/mmm$ <sup>a</sup>**

	$MgB_2$	$MgB_{1.98}C_{0.02}$	$MgB_{1.96}C_{0.04}$	$MgB_{1.94}C_{0.06}$		$MgB_{1.92}C_{0.08}$		$MgB_{1.90}C_{0.10}$	
				phase 1	phase 2	phase 1	phase 2	phase 1	phase 2
$a$ (Å)	3.08208(2)	3.07901(2)	3.07513(2)	3.07640(9)	3.06744(5)	3.07436(8)	3.06224(3)	3.07314(6)	3.05776(7)
$c$ (Å)	3.51404(7)	3.51321(4)	3.51460(4)	3.51640(14)	3.51502(7)	3.51789(13)	3.51501(5)	3.51864(7)	3.51345(9)
fraction (%)	83(1)	84.3(6)	100	31.8(5)	68.2(5)	28.6(3)	71.4(3)	57.2(3)	42.8(3)
occupancy on the B site	0.092(8)	0.098(8)	0.074(8)	0.028(30)	0.124(16)	0.028(26)	0.168(12)	0.008(16)	0.140(24)
$R_{wp}$ (%)	6.82	7.27	8.78	7.43		6.89		7.33	
$\chi^2$	2.84	3.49	5.33	3.77		3.35		2.96	

<sup>a</sup> The atoms were placed in the following positions in the unit cell: Mg in 1a (0, 0, 0); B in 2d (1/3, 2/3, 1/2).

reproduced using two  $MgB_{2+\delta}$  phases that only differ in their  $c$  lattice constants. In the following, only the data related to the main phase (relative weight larger than 80%; Table 1) are presented. The lattice constants for  $MgB_2$  were determined to be  $a = 3.082\ 08(2)$  Å and  $c = 3.514\ 04(7)$  Å at 16 K, consistent with literature data.<sup>9,24</sup> Figure 1a shows the results of the Rietveld refinement for the  $MgB_{1.98}C_{0.02}$  sample (agreement factors:  $R_{wp} = 7.27\%$ ,  $\chi^2 = 3.49$ ).

For the other  $MgB_{2-x}C_x$  compositions, all main reflections can still be indexed within the  $P6/mmm$  space group. However, a closer examination of the diffraction profiles at both 16 K and room temperature shows that the  $(hk0)$  lines are split for carbon contents equal to or higher than 0.06 (inset of Figure 1b), whereas the width of the  $(00l)$  reflections remains virtually unchanged. In addition, the double peaks present have different widths, so that they reflect the presence of a second phase of the same  $AlB_2$ -type crystal structure rather than the occurrence of a structural phase transition associated with crystal symmetry reduction. Note that the additional phase cannot be assigned to the tetragonal  $MgC_2$  end member.<sup>25</sup> The diffraction pattern of  $MgB_{1.96}C_{0.04}$  does not reveal any splitting of the  $(hk0)$  reflections even at high angles. However, increased line widths are evident when compared with those of the  $MgB_{1.98}C_{0.02}$  sample. A Williamson–Hall analysis of the diffraction profile is consistent with the conclusion that this composition is close to the onset of phase separation.<sup>26</sup>

The diffraction profiles for  $x \geq 0.06$  were subsequently refined using two  $MgB_{2+\delta}$  phases, with similar interlayer separations but quite different in-plane lattice parameters. Lattice constants, relative phase fractions, independent profile parameters, and occupancies of the boron site,  $\delta$ , were included in the refinement. The influence of the zero shift was found to be negligible. A single overall thermal factor,  $B$ , of  $0.19\ \text{\AA}^2$ , determined from the refinements on the undoped sample, was used for all phases. Figure 1b displays the X-ray refinement of the diffraction profile for  $MgB_{1.94}C_{0.06}$  at 16 K (agreement factors:  $R_{wp} = 7.43\%$ ,  $\chi^2 = 3.77$ ). The lattice constants were determined to be  $a = 3.067\ 44(5)$  Å and  $c = 3.515\ 02(7)$  Å for the majority (68%) and  $a = 3.076\ 40(9)$  Å and  $c = 3.516\ 40(14)$  Å for the minority (32%) phase. The results of the analyses are summarized in Table 1.

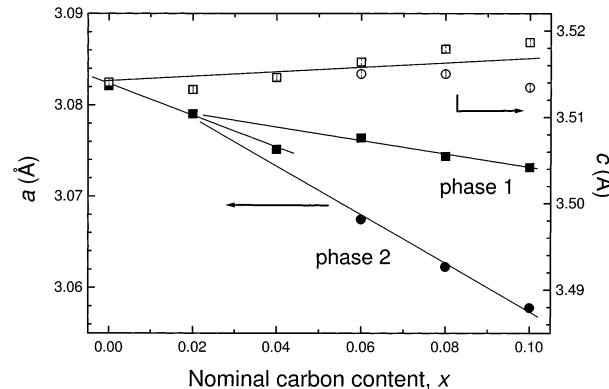


**Figure 2.** Lattice constants at 16 K as a function of the nominal carbon content,  $x$ , in the  $MgB_{2-x}C_x$  series ( $0 \leq x \leq 0.1$ ).

Figure 2 shows the as-extracted lattice parameters plotted as a function of the nominal carbon content,  $x$ . Because resolution of the coexisting phases has not been possible for  $MgB_{1.96}C_{0.04}$ , an averaged structure was derived from the refinements. Figure 2 implies the presence of macroscopic phase separation at an extremely low carbon doping level, on the order of  $x \approx 0.04$ . At higher carbon contents, two phases are present that differ mainly in their in-plane lattice constants. Their  $c$  parameters remain almost identical with that of  $MgB_2$ . Surprisingly, the  $a$  lattice constants of phases 1 and 2 gradually decrease with increasing nominal carbon content as for an extended solid solution behavior, suggesting that one of the two (or both) phase(s) do(es) not contain any carbon. Their lattice constants should then reflect a  $MgB_{2-\delta}$  chemical composition. However, previous structural analyses have shown an increased interlayer separation for compositions that present a deficit in boron, while the  $a$  parameter is virtually unaffected, in opposition to what is observed here. In addition, our refinements of the boron occupancy systematically indicate an electron excess ( $\delta/2$  per B site) rather than a deficit. Carbon is, therefore, present in the boron layers for both phases but in different concentrations: phase 2 is richer in carbon than phase 1. The structural analyses are in agreement with  $ac$  susceptibility measurements, which show the presence of more than one peak in the  $\chi''-T$  dependence of  $MgB_{2-x}C_x$  for  $x > 0.04$  and imply the coexistence of two (or more) phases with different  $T_c$ 's.<sup>27</sup>

Assuming a linear variation of the  $a$  lattice constants with carbon concentration, as suggested by Figure 2 for

(24) Jorgensen, J. D.; Hinks, D. G.; Short, S. *Phys. Rev. B* **2001**, 63, 224522.

(25) Bredig, M. A. *J. Am. Chem. Soc.* **1943**, 65, 1482.

(26) Maurin, I.; Margadonna, S.; Prassides, K.; Takenobu, T.; Ito, T.; Chi, D. H.; Iwasa, Y.; Fitch, A. N. *Physica B* **2002**, 318, 392.

(27) Papagelis, K.; Arvanitidis, J.; Margadonna, S.; Iwasa, Y.; Takenobu, T.; Pissas, M.; Prassides, K. *J. Phys.: Condens. Matter* **2002**, 14, 7363.

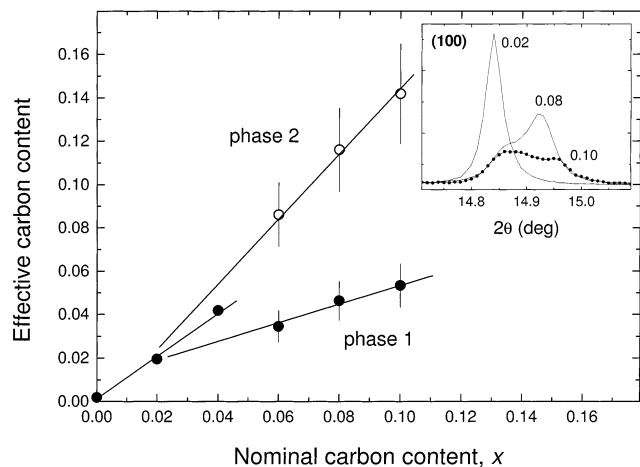


**Figure 3.** Effective carbon content derived from the linear variation of the  $a$  lattice constant with the carbon concentration in the boron sheets (Figure 2), as a function of the nominal carbon concentration in the  $MgB_{2-x}C_x$  series. Inset: the (100) reflection for selected compositions.

$x \leq 0.04$ , we attempted to estimate the effective carbon content of phases 1 and 2 in the various samples (Figure 3). However, the total carbon content in the multiphase samples, deduced from the chemical formula of phases 1 and 2 and their relative weight (Table 1), is then always larger than the overall nominal C doping level. Hence, either the linearity, established on a small number of data points, or the two-phase model is not strictly valid. The latter hypothesis is supported by the analysis of the diffraction line broadenings: for  $x \geq 0.06$ , the width, shape, and asymmetry of the ( $hk0$ ) reflections are quite different between phases 1 and 2, suggesting that these highly doped samples probably consist of more than two phases. At least three phases should be present in  $MgB_{1.90}C_{0.10}$ , as evidenced by the complex peak shape of the ( $hk0$ ) lines (inset of Figure 3).

The multiphase behavior at high carbon doping levels may account for a bimodal distribution of carbon concentrations, for instance, related to spinodal decomposition. An alternative explanation would involve a set of well-defined compositions and requires systematic ordering phenomena, as in the Al-doped series.<sup>16,17</sup> Ordering of the dopants may arise from elastic interaction between defects that tend to localize them, as supported by the difference in atomic radii between C and B of ca. 15%. The minimization of their repulsion then leads to an energy gain larger than the entropy,  $-T dS$ , associated with a random (solid solution) distribution of carbon atoms within the boron sheets. The absence of superstructure peaks in the diffraction profiles does not rule out such a hypothesis. Finally, we note that the apparent formation of two (or more) solid solutions in the three-component system, Mg, B, and C, will be contrary to Gibbs' phase rule. However, for phase rules to be applied under equilibrium conditions, all reaction products need to be taken into account, and in the present system, formation of  $MgO$  and other

minor unidentified impurities renders detailed thermodynamic considerations extremely complex. Nonetheless, the multiphase behavior on doping may well originate for kinetic reasons; namely, the difference in the diffusion coefficients of B and C at the reaction conditions could be the main cause of the observed inhomogeneities and pseudo-solid-solution behavior in the bulk samples.

The present results clearly show the complexity of the substitutional chemistry in  $MgB_2$  and demonstrate the utility of high-resolution structural studies. We suspect that the miscibility range of other dopants reported in the literature is also much narrower than what has been derived by low-resolution structural measurements. For instance, our preliminary high-resolution data for the  $Mg_{1-x}Al_xB_2$  series show a phase separation onset as low as  $x = 0.025$ ,<sup>28</sup> significantly lower than what was reported in the literature.<sup>10</sup> The near coincidence of the doping level at which phase separation occurs in  $MgB_{2-x}C_x$  and  $Mg_{1-x}Al_xB_2$  (between 2 and 3% of electron doping of the conduction band) raises the issue that it may be driven by electronic reasons. Further experiments are necessary to explore these effects in doped  $MgB_2$  phases, especially because an electronic origin of the behavior will have important implications for the mechanism of superconductivity in these materials.

#### 4. Conclusions

In conclusion, high-resolution synchrotron X-ray diffraction measurements have been carried out on the electron-doped  $MgB_{2-x}C_x$  series. A splitting of the ( $hk0$ ) lines for  $x \geq 0.04$  indicates an extremely small miscibility of carbon within the boron sheets of  $MgB_2$  under the present synthetic conditions. Above this solubility limit, macroscopic phase separation occurs, leading to coexisting phases with the same  $AlB_2$  hexagonal structure that differ in their in-plane lattice constants and thus in their carbon-doping levels. The microscopic model for the observed multiphase behavior is still not clear and may involve a continuous distribution of carbon doping with a strongly bimodal repartition that might be reminiscent of spinodal-like decomposition or ordering of the carbon atoms in the B sheets due to elastic interactions, or it may arise from kinetic effects associated with the differing diffusivities of B and C. Because phase separation occurs for a similar electron-doping level in both  $MgB_{2-x}C_x$  and  $Mg_{1-x}Al_xB_2$ , the multiphase behavior may alternatively have an electronic origin.

**Acknowledgment.** We thank one of the reviewers for pertinent comments, the Royal Society (U.K./Japan CRP) for financial support, Jesus College (Cambridge) for a Research Fellowship to S.M., and the ESRF for provision of synchrotron X-ray beamline time.

CM020308K

(28) Pissas, M.; Papavassiliou, G.; Karayanni, M.; Fardis, M.; Maurin, I.; Margioliaki, I.; Prassides, K.; Christides, C. *Phys. Rev. B* **2002**, *65*, 184514.